The Drift of Magnetic Vortices in a Random Field of Anchoring Centers

Vitaly Orlov[1,2], Anatoly Ivanov[1], Irina Orlova[3], and Gennady Patrin[1,2]

[1]Institute of Engineering Physics and Radio Electronics, Siberian Federal University, 660041 Krasnoyarsk, Russia
[2]Kirensky Institute of Physics, Federal Research Center KSC SB RAS, 660036 Krasnoyarsk, Russia
[3]Institute of Mathematics, Physics and Informatics, Krasnoyarsk State Pedagogical University named after V. P. Astafyev, 660049 Krasnoyarsk, Russia

This article theoretically solves the problem of the thermally activated motion of gas of non-interacting magnetic vortices/skyrmions in the field of defects located randomly, i.e., anchoring centers. The properties of the anchoring centers can also fluctuate. The factor that drives the gas of quasiparticles can be of any physical nature (fields, currents, gradients of the magnetic characteristics of the magnet, and so on). The process of vortices motion is described as a sequence of thermally activated separation of vortices from the attracting centers. The cases of some model distribution functions of the energy barriers are considered: 1) the barriers are of the same height; 2) the heights of the barriers are distributed evenly; and 3) the heights are distributed according to the normal law. Within these models, analytical expressions for the drift velocity and the diffusion gas coefficient of quasiparticles are obtained.

Index Terms—**Magnetic nanostripes, magnetic vortex, pinning, skyrmion.**

I. Introduction

AT PRESENT, the magnetic objects that are characterized by a special state of magnetization, i.e., magnetic excitations in the form of vortex structures (magnetic vortices, skyrmions, and vortex domain walls), are being studied with great interest. It is connected with the possibility to use them as a basis for general-purpose sensors, fast and reliable information storage systems, and other spintronics devices. The reasons why in this context the interest is focused on vortex structures are related to the special physical properties of these objects.

Under certain conditions, the state of magnetization in a magnetic vortex is quite stable, and the methods of controlling this state are sufficiently developed. It allows considering the structures with a vortex distribution of magnetization as promising variants of information carriers of the new generation. The state of magnetization of an individual vortex can be identified with a bit of information. Moreover, the distribution of magnetization in a magnetic vortex can be characterized by two parameters: the $p = \pm 1$ polarity, which sets the direction of the magnetic moment of the vortex core (along or against the selected axis) and the $q = \pm 1$ chirality, i.e., the circulation of magnetization around the selected axis (clockwise or anticlockwise). The state of each of the p and q parameters, or a combination of them, sets a value of more than one bit on a single vortex/skyrmion. This circumstance gives hope for the creation of devices with a high recording density without the loss of information storage reliability in the near future.

Ferromagnetic nanofilm is one of the most promising objects for spintronics devices. Such a nanofilm may contain a swarm of such vortices [1]–[13]. The state of vortices can be controlled by both external fields and spin-polarized currents (see [14]–[16]) and even by mechanical stress gradients (for example, [17] and [18]). The stability of the vortex distribution of magnetization is determined by the thickness of the magnetic film [19], so the thickness of the nanofilms should satisfy the requirement of the stability of the vortex distribution.

In theoretical descriptions of the dynamics of a vortex magnetic structure, the method of collective variables in the rigid vortex model [20]–[22] proved to be productive. In this case, the coordinate and velocity of the center, i.e., the core of the vortex, are used as parameters that characterize the state of the vortex, and the distribution of magnetization inside the vortex is considered to be practically unchanged. The core is the central part of the vortex with a strongly inhomogeneous distribution of magnetization going out from the plane of the magnet. Subsequently, this approach has been successfully developed and exploited by many authors (see [23]–[28]). Within this approach, the Lagrangian of the magnetic subsystem is used to obtain the equation of motion of the magnetic vortex as a quasiparticle in the form

$$\mathbf{G}_3 \times \ddot{\mathbf{v}} + \widehat{\mu}\dot{\mathbf{v}} + \mathbf{G} \times \mathbf{v} + \widehat{D}\mathbf{v} + \nabla W = 0. \tag{1}$$

$\mathbf{G}$ and $\mathbf{G}_3$ are gyrovectors of the first and third orders, respectively [20], [25]–[27], perpendicular to the plane of the magnet. $\mathbf{v}$ is the velocity of the core. W is the potential energy possessed by the vortex.

$\widehat{D}$ and $\widehat{\mu}$ are the tensors of the effective coefficients of the friction force and the effective mass of the vortex, respectively. The points above the vectors mean the time differentiation. Thus, it is possible to describe the dynamics of magnetic vortices as particles moving under the action of forces, according to (1). The core size is on the order of tens of nanometers.

Due to the small size of the vortex core and its small mass $M_{\text{vort}} \sim 10^{-22}$ kg [29]–[31], the thermal random walk of the vortices similar to the Brownian [32]–[36] is

Manuscript received May 25, 2021; revised October 6, 2021 and January 18, 2022; accepted March 11, 2022. Date of publication March 16, 2022; date of current version April 25, 2022. Corresponding author: V. Orlov (e-mail: vaorlov@sfu-kras.ru).

Color versions of one or more figures in this article are available at https://doi.org/10.1109/TMAG.2022.3160008.

Digital Object Identifier 10.1109/TMAG.2022.3160008

essential. Some ideas about the nature of such motion have already been formed for particles with zero values of $\mathbf{G}_3$ and $\widehat{\mu}$ [37]–[39]. In particular, it is shown that the standard deviation of a particle increases over time according to the Einstein–Smoluchowski law with a coefficient determined by the expression

$$\chi = k_B T \frac{D}{G^2 + D^2} \tag{2}$$

where k_B is Boltzmann's constant and T is the temperature.

In some real situations, the motion of vortices/skyrmions cannot be considered as motion in a homogeneous matrix. In thin low-dimensional magnets (nanowires and nanostripes), as a rule, there are defects that create a random or modulated force field (see [40] and [40]), where the vortex moves like a particle. It is especially important to accept the factor of inhomogeneous force field in polycrystalline magnets or composites. Therefore, more and more attention has recently been paid to the effects of the interaction of vortices–quasiparticles with inhomogeneities of the magnetic structure. The inhomogeneities may be presented by the surface defects of the magnet, fluctuations in local anisotropy, changes in the magnetic properties in the complex at the boundaries of different magnetic phases, and so on (see [42]–[48] and [51]).

It is obvious that the interaction of vortices/skyrmions with inhomogeneities of the matrix where the swarm of quasiparticles moves significantly affects the behavior of the system. Therefore, the study of the gas vortices dynamics in the field of anchoring centers that prevent movement is of great interest. It is reasonable to expect that the sliding of quasiparticles is similar to the thermally activated movement of dislocations or domain walls.

Thermally activated motion due to thermal rattling (accompanied by breakdowns from the anchoring centers and rapid movement between them) is the predominant mechanism for the gas propagation of quasiparticles through a magnet [52]. The method that is actively used to describe the kinetics of chemical reactions, which is based on the Arrhenius law, is productive to study such a motion. We will use this law later to set the waiting time for the jump of the vortex to the next anchoring center.

The interaction of vortex structures with magnetic inhomogeneities shows a variety depending on the type and configuration of the defect. The potential of such interaction can result in both the reflection of the vortex core from the defect and its capture. The vortex fixation can be realized, for example, on inhomogeneities of magnetic anisotropy (fluctuations in the direction of the local axis or the anisotropy constant) both point and extended [51], [53]–[56].

Thus, the core of the magnetic vortex/skyrmion near the magnetic inhomogeneity or directly on it behaves as a quasiparticle in the energy well-formed by the potentials of the defect [57] and external forces (if any). Fig. 1 shows the nanofilm model that is considered in this article with linear randomly arranged defects. In the depicted model, the anchoring centers are linear extended defects oriented perpendicular to the long axis of the tape and creating potentials that prevent the movement of the vortex along the x-axis. It is obvious that, in the most general case, not only the coordinates

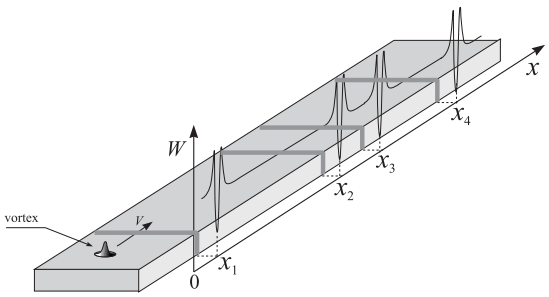

Fig. 1. Model of a nanofilm with a schematically shown distribution of the potential energy of the vortex depending on the coordinate. The inhomogeneity of the potential can be caused by inhomogeneities of the magnetic structure of the magnet in the x_1, x_2, x_3, ... coordinates.

of the anchoring centers are random but also their other characteristics: the profiles of potential barriers, their heights, and their length.

The fluctuations in the magnetic parameters of defects significantly complicate the theoretical analysis of the nature of the magnetic vortices motion, so, in order to obtain practically significant results, computer modeling is often resorted to (see [58]–[60]).

In this article, we present a statistical description of the time evolution of a conglomerate of magnetic vortices/skyrmions as a gas of non-interacting quasiparticles involved in 1-D motion in the field of magnetic structure defects under the influence of a constant external force. The approximation of isolated quasiparticles is justified in the case of their low concentration if the nature of their interaction is short range (the case of skyrmions). The nature of the interaction of magnetic vortices is long range. However, the model of gas of non-interacting vortices is applicable for temperatures above some critical T_{KT}, above which the nature of the interaction is short range [61], [62]. In addition, we will assume that the barrier heights are much greater than the interparticle interaction energy.

For the needs of spintronics, it is precisely systems with an average distance between vortices that are so large that the influence of neighboring cores on each other's magnetic states is of interest. This motion can serve as a model for the gas propagation of vortices (skyrmions and vortex domain walls) in ferromagnetic inhomogeneous nanofilms. The main task is to describe the development with the time distribution of random coordinates of the vortex cores.

II. Evolution of the Spatial Distribution of the Vortex Gas in the Field of Identical Defects (Model 1)

To describe the nature of the vortices displacement under the influence of a driving force in a random field of defects, we calculate the average number of trajectories of the $\rho(x, t)$ cores, resulting in a favorable outcome, i.e., the core is in the x-coordinate at the t time. Let the core be located at the origin of the coordinates at the initial moment of time. It is important to note that the free movement of magnetic vortices in a magnet in the absence of a driving force is impossible [61]–[63], unlike skyrmions. In addition, the force under which the vortex moves is so great that, as a result of the thermal motion, the jumps of the cores in the opposite direction are quite rare and do not affect the resulting drift motion.

Under the action of the driving force, the quasiparticles break off the defect and begin to move, which can have a complex character. However, within a short time, due to damping, a steady state occurs. In this mode, the trajectory of the core asymptotically tends to the direction along the x-axis. However, depending on the chirality/polarity, these trajectories gravitate toward the side surfaces of the nanostripe. This phenomenon follows from (1); it is well known and is called the skyrmion Hall effect. Thus, in the interval from defect to defect, the motion of quasiparticles is practically rectilinear and uniform. Moreover, the times of movement of the cores between the anchoring centers are negligible for the times when the vortices are in a bound with defects.

Indeed, the constant component of the force acts on the vortex, the thermal rattle in the local minimum of the potential energy is not symmetric, and the vortex disruption in the direction of the force action is preferred (see Fig. 2). Let us take an elementary event: the core is in the x-coordinate at the t time. It has born a thermally activated disruption from certain obstacles in the number of n pieces at certain time points from the corresponding intervals; they are dx_k and dt_k. The probability of such an elementary event can be written as

$$dP_n^{(el)}(x,t) = \prod_{k=1}^{n} \rho(\Delta x_k)\rho(\Delta t_k)\rho(W_k)dx_k dt_k dW_k \times \delta\left(x - \sum_{k=1}^{n} \Delta x_k\right)\delta\left(t - \sum_{k=1}^{n} \Delta t_k\right). \quad (3)$$

The notations that have been introduced are as follows: $\Delta x_k = x_k - x_{k-1}$ is the increment of the core coordinate as a result of the jump; $\Delta t_k = t_k - t_{k-1}$ is the time taken to move the core between neighboring anchoring centers; W_k is the height of the energy barrier with the k number; $\rho(W_k)$ is the density of the distribution of the barriers' heights

$$\rho(\Delta x_k) = \mu e^{-\mu \Delta x_k}, \quad \rho(\Delta t_k) = \nu_k e^{-\nu_k \Delta t_k} \quad (4)$$

are the distribution densities of the jump lengths and their durations, respectively (Poisson's law); μ is the linear coordinate density of the distribution of the anchoring centers; and ν_k is the frequency of attempts of the core disruption from the defect, which is determined by the Arrhenius law

$$\nu_k = \nu_0 \exp\left(-\frac{W_k}{k_B T}\right). \quad (5)$$

The ν_0 constant, as a rule, has the frequency order of the ferromagnetic resonance in the magnet. The Dirac functions in expression (3) select from the variety of distributions of x_k-coordinates and the t_k moments of time only those that satisfy the condition that the vortex hits the x final coordinate by the t time.

It is important to note that the values of the frequency ν_k, ν_0, and energy W_k are determined by the physical characteristics of magnetic vortices, such as the effective mass, the profile of the magnetization distribution functions, and the size of the core.

To calculate the probability of a complex event of hitting the x-coordinate by the t time, it is necessary to sum expression (3) over all possible configurations $\{W_k, x_k, t_k\}$ that lead

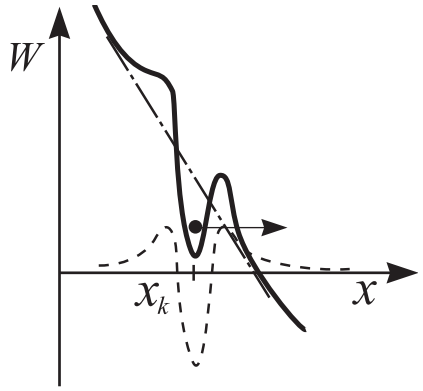

Fig. 2. Scheme of the potential of the anchoring center without an external force (dashed curve). The dashed inclined line shows the contribution to the potential energy from an external factor. Superimposing a straight line distorts the symmetric potential (solid curve), resulting in a preferred jump of the particle (shaded circle) in the direction indicated by the arrow.

to a favorable result

$$dP_n(x,t) = \int_{W_n} \cdots \int_{W_1} \int_0^t \cdots \int_0^{t_2} \int_0^x \cdots \int_0^{x_2} dP_n^{(el)}(x,t). \quad (6)$$

Here, due to the vortex drift mainly in the positive direction of the x-axis, the integration is performed according to the scheme: x_1 from 0 to x_2, then x_2 from 0 to x_3, and so on. As a result, we obtain

$$\frac{dP_n(x,t)}{\mu dx} = \frac{(\mu x)^{n-1} e^{-\mu x}}{(n-1)!} \times \int_{W_n} \cdots \int_{W_1} \int_0^t \cdots \int_0^{t_2} \prod_{k=1}^{n} \rho(\Delta t_k)\rho(W_k) dt_k dW_k \times \delta\left(t - \sum_{k=1}^{n} \Delta t_k\right). \quad (7)$$

Further calculation (7) for an arbitrary distribution $\rho(W_k)$ is not possible due to the connection of functions (4) and (5) in the general case, but it is permissible for the special case of the same energies of all anchoring centers $W_k = W_0$. For this case, the energy distribution density is described by the Dirac function: $\rho(W_k) = \delta(W_k - W_0)$ with $\int_0^\infty \delta(W_k - W_0) dW_k = 1$. Then, the integration over t_k time points is significantly simplified and follows the same scheme as the integration over coordinates. As a result, for (7), we obtain

$$\frac{dP_n(x,t)}{(\mu dx)(\nu dt)} = \frac{(\mu x \nu t)^{n-1} e^{-\mu x - \nu t}}{(n-1)!^2} = \rho_n(x,t). \quad (8)$$

The $\rho_n(x,t)$ value can be given the meaning of the dimensionless density of the number of possible trajectories (in the $\{W, x, t\}$ configuration space), resulting in the vortex core is in the x-coordinate at the t time and breaking off from the n anchoring centers.

To calculate the final expression for $\rho(x,t)$ for all possible n, it is necessary to sum

$$\rho(x,t) = \sum_{n=1}^{\infty} \rho_n(x,t). \quad (9)$$

For an approximate calculation (8), we replace the summation with integration and use Stirling's formula to represent the factorial by means of analytical functions

$$\rho(x,t) \approx \frac{1}{2\pi} e^{-\mu x-\nu t} \sum_{n=1}^{\infty} \frac{\left(\mu x \nu t e^2\right)^{n-1}}{(n-1)^{2n-1}} \approx \frac{1}{2\pi} e^{-\mu x-\nu t} \int_0^{\infty} \frac{\left(\mu x \nu t e^2\right)^{n-1}}{(n-1)^{2n-1}} dn. \tag{10}$$

The sum in (10) contains a large number of random terms; in addition, these terms are fairly well localized by functions from n. Therefore, according to the central limit theorem, this sum can be considered extremely close to the Gaussian function. This allows us to attempt to reduce the integral in (10) to an exponential form with the expansion of the integrand to terms of the second order of smallness relative to some n_0 corresponding to the maximum of the integral

$$\begin{aligned}
&\int_0^{\infty} \frac{\left(\mu x \nu t e^2\right)^{n-1}}{(n-1)^{2n-1}} dn \\
&= \int_0^{\infty} \exp\left(\ln\left(\frac{\left(\mu x \nu t e^2\right)^{n-1}}{(n-1)^{2n-1}}\right)\right) dn \\
&\approx \int_{-\infty}^{\infty} \left(\exp\left((n_0-1+\xi)\ln\left(\mu x \nu t e^2\right)\right.\right. \\
&\qquad -(2n_0-1+2\xi) \\
&\qquad \left.\left.\times\left(\ln(n_0-1)+\frac{\xi}{n_0-1}-\frac{\xi^2}{2(n_0-1)^2}\right)\right)\right) d\xi \\
&= \frac{n_0^{2n_0-2} e^{2(n_0-1)}}{(n_0-1)^{2n_0-1}} \int_{-\infty}^{\infty} \exp\left(-\xi^2 \frac{2n_0-3}{2(n_0-1)^2}\right. \\
&\quad \left.+\xi\left(2+2\ln\left(\frac{n_0}{n_0-1}\right)-\frac{2n_0-1}{n_0-1}\right)\right) d\xi \\
&= \sqrt{\frac{\pi}{n_0}} \left(\frac{n_0}{n_0-1}\right)^{2n_0-1} e^{2(n_0-1)} \approx \sqrt{\frac{\pi}{n_0}} e^{2n_0}.
\end{aligned} \tag{11}$$

Here, we use the $n_0 \gg 1$ condition. The value of the n_0 parameter corresponding to the extremum of integrand (10), with (8), is determined by the obvious equality

$$\frac{\left(\mu x \nu t e^2\right)^{n-1}}{(n-1)!^2} = \frac{\left(\mu x \nu t e^2\right)^{n}}{n!^2}. \tag{12}$$

It is obtained

$$n_0 = \sqrt{\mu x \nu t}. \tag{13}$$

With (11) and (13) for function (10), it is obtained

$$\rho(x,t) = \frac{1}{\sqrt{4\pi\left(\mu x \nu t\right)^{\frac{1}{2}}}} e^{-\left(\sqrt{\mu x}-\sqrt{\nu t}\right)^2}. \tag{14}$$

This function actually shows the evolution of the spatial distribution of the vortex/skyrmion gas over time.

Surface (14) is shown in Fig. 3. The coordinate distribution has an obvious maximum, which moves in the direction of the force action over time and is smoothed out (the half-width of the bell increases). This can be interpreted as follows. At the initial time, a large number of vortex cores (gas) are collected at the initial coordinate. After actuating the force and starting the countdown, the gas begins to spread through the magnet,

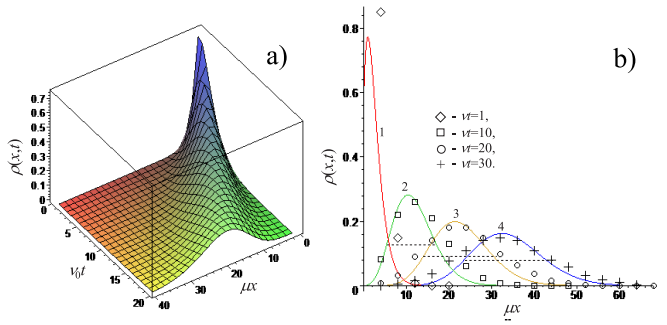

Fig. 3. (a) Distribution of the vortex gas depending on the coordinate and time. To demonstrate the evolution of the coordinate distribution, (b) shows sections of the $\rho(x,t)$ surface at some moments of time. The dashed lines show the half-widths of the distributions that mean an increase in the dispersion of the coordinates of the quasiparticles over time. The curves are plotted at the following time points: 1—$\nu t = 1$; 2—$\nu t = 10$; 3—$\nu t = 20$; and 4—$\nu t = 30$. Hereinafter, the dots show the results of modeling the gas vortex propagation by the Metropolis method taking into account the Arrhenius law (up to a factor of the order of unity).

bearing thermal activated jumps. The most probable velocity V of particle flow can be easily calculated by examining distribution (14) for extremum

$$V = \frac{\nu}{\mu} = \frac{\nu_0}{\mu} \exp\left(-\frac{W_0}{k_B T}\right). \tag{15}$$

At the same time, due to the random nature of the acts of disruption from the anchoring centers, the dispersion of the spatial distribution of particles increases. The growth of the spread of the coordinates of the quasiparticles gas can be estimated as the half-width of the distribution (14). The $\rho(x,t)$ maximum value at the t time with (15) is equal to $\sim 1/(4\pi\nu t)^{1/2}$. Then, the coordinate values that correspond to the half of the bell height $\rho(x,t)$ are determined by the following equation:

$$\frac{1}{\sqrt{4\pi\left(\mu x \nu t\right)^{\frac{1}{2}}}} e^{-\left(\sqrt{\mu x}-\sqrt{\nu t}\right)^2} = \frac{1}{2} \frac{1}{\sqrt{4\pi\nu t}}. \tag{16}$$

The analytical solution of (17) is possible under the $(\sqrt{\mu x}-\sqrt{\nu t}) \ll 1$ assumption, i.e., in a relatively long time after the start of the movement. When the stationary mode of motion begins for the variance of the coordinates, we obtain

$$\sigma_x^2 = (\Delta x)^2 \approx 16\ln(2)\frac{\nu_0 t}{\mu^2} \exp\left(-\frac{W_0}{k_B T}\right). \tag{17}$$

Furthermore, we consider a more general case of the chaotic distribution of the W_k energy barriers' heights. Due to the difference in the W_k energies, the integration over the t_k times of expression (7) is so difficult that this procedure loses its practical meaning. At the same time, understanding that the $\rho(x,t)$ function is localized and close to the normal distribution (due to the validity of the central limit theorem) allows us to advance in approximate calculations.

We expect that the $\rho(x,t)$ deviation from the normal distribution is insignificant, but they can also be minimized by using the refinement technology described, for example, in [64] and [65]. The principle of the method is the identical multiplication of the calculated function by the exponent containing the α fitting parameter, which depends on the x and t arguments of the $\rho(x,t)$ desired function. This parameter is

then selected so that the desired function is best approximated to the maximum of the normal distribution. It is in this case that we allow the minimum error of the $\rho(x,t)$ calculating. Later, we will operate only with the integral part of the expression (7)

$$I_n = \int_{W_n}\cdots\int_{W_1}\int_0^t\cdots\int_0^{t_2}\prod_{k=1}^{n}\rho(\Delta t_k)\rho(W_k)dt_k dW_k \times\delta\left(t-\sum_{k=1}^{n}\Delta t_k\right). \quad (18)$$

We change the expression as follows:

$$I_n = e^{-\alpha t}I_n^*,\quad I_n^* = I_n e^{\alpha t}. \quad (19)$$

Then, we perform an approximate calculation of I_n^* similar to the proof of the central limit theorem. The Fourier image of the I_n^* value with (4) is as follows:

$$\begin{aligned}\Omega(\omega,\alpha) &= \int_0^\infty e^{i\omega t}I_n^* dt\\ &= \int_{W_n}\cdots\int_{W_1}\int_0^t\cdots\int_0^{t_2}\prod_{k=1}^{n}\rho(\Delta t_k)\rho(W_k)e^{(i\omega+\alpha)\Delta t_k}dt_k dW_k\\ &= \prod_{k=1}^{n}\int_W\int_0^t\rho(W_k)\nu_k e^{(i\omega+\alpha-\nu_k)t_k}dt_k dW_k. \end{aligned}\quad (20)$$

If we assume that the activation energies of all the anchoring centers are distributed according to the same laws, then multiple integral (20) can be represented as the product of the same type of integrals

$$\Omega(\omega,\alpha) = u^n(\omega,\alpha). \quad (21)$$

The notation is introduced

$$u(\omega,\alpha) = \int_W\int_0^t \nu\rho(W)e^{(i\omega+\alpha-\nu)t}dtdW \approx \int_W\frac{\nu\rho(W)}{\nu-i\omega-\alpha}dW. \quad (22)$$

Then, calculation (22) in the Gaussian approximation is performed

$$\begin{aligned}\Omega(\omega,\alpha) &= \exp(n\ln(u(\omega,\alpha)))\\ &\approx u^n(0,\alpha)\exp\left(-\omega^2\frac{n}{2}\frac{\partial^2\ln(u)}{\partial(i\omega)^2}\bigg|_{\omega=0} + i\omega n\frac{\partial\ln(u)}{\partial(i\omega)}\bigg|_{\omega=0}\right). \end{aligned}\quad (23)$$

After the inverse Fourier transformation, for integral (19), it is obtained

$$\begin{aligned}I_n &= \frac{e^{-\alpha t}}{2\pi}\int e^{-i\omega t}\Omega(\omega,\alpha)d\omega\\ &= \frac{u^n(0,\alpha)e^{-\alpha t}}{\sqrt{4\pi\sigma^2}}\exp\left(-\frac{(t-t_0)^2}{2\sigma^2}\right). \end{aligned}\quad (24)$$

It can be written for expression (7) with (24)

$$\rho_n(x,t) = \frac{u^n(0,\alpha)(\mu x)^{n-1}e^{-\mu x-\alpha t}}{(n-1)!} \times\frac{1}{\sqrt{4\pi\sigma^2}}\exp\left(-\frac{(t-t_0)^2}{2\sigma^2}\right). \quad (25)$$

The notations are introduced

$$t_0 = n\frac{\partial\ln(u)}{\partial\omega}\bigg|_{\omega=0},\quad \sigma^2 = n\frac{\partial^2\ln(u)}{\partial(i\omega)^2}\bigg|_{\omega=0}. \quad (26)$$

The minimum error of the Gaussian approximation is achieved if $t = t_0$. Then, for (9), we get

$$\rho(x,t) = \sum_{n=1}^{\infty}\frac{u^n(0,\alpha)(\mu x)^{n-1}e^{-\mu x-\alpha t}}{\sqrt{4\pi\sigma^2}(n-1)!}. \quad (27)$$

The α fitting parameter is defined from the condition

$$t = n_0\frac{\partial\ln(u)}{\partial\omega}\bigg|_{\omega=0}. \quad (28)$$

Here, n_0 is defined by scheme (12).

The final expression for $\rho(x,t)$ is calculated similar to reasoning (10)–(14). As a result, we get

$$\begin{aligned}\rho(x,t) &\approx \frac{u_0}{\sqrt{4\pi\sigma^2}}e^{-\mu x-\alpha t+n_0},\quad n_0 = \mu x u_0\\ u_0 &= \int_W\frac{\nu\rho(W)dW}{\nu-\alpha}. \end{aligned}\quad (29)$$

Expression (29) is easy to test on the case of non-fluctuating barrier heights: $\rho(W) = \delta(W-W_0)$ and $\nu = \nu_0\exp(-W_0/(k_BT))$. As a result, from (28) and (29), we get $\alpha = \nu - (\mu x\nu/t)^{1/2}$, $u_0 = (\nu t/(\mu x))^{1/2}$, $n_0 = (\mu x\nu t)^{1/2}$, and $\sigma^2 = t^2/(\mu x\nu t)^{1/2}$; therefore, the expression for $\rho(x,t)$ is exactly the same as the result previously obtained (14).

Then, the general rule (28) and (29) is used to calculate the nature of the movement of the quasiparticles gas in situations closer to the reality of the fluctuating height of the W energy barriers.

III. Smooth Distribution of Activation Energy (Model 2)

In this section, we consider a model of a magnet where the activation energy of the anchoring centers is distributed evenly in the $W_1,\ldots,W_2$ range. For the energy distribution density, we have $\rho(W) = 1/(W_2-W_1) = \rho_0$; then, for (22), we get

$$\begin{aligned}u(\omega,\alpha) &= \int_{W_1}^{W_2}\frac{\nu_0\rho_0\exp(-W/(k_BT))dW}{\nu_0\exp(-W/(k_BT))-i\omega-\alpha}\\ &= \rho_0 k_BT\ln\left(\frac{i\omega+\alpha-\nu_0\exp(-W_1/(k_BT))}{i\omega+\alpha-\nu_0\exp(-W_2/(k_BT))}\right). \end{aligned}\quad (30)$$

First, the value of the α fitting parameter is determined. For this purpose, it is necessary to return to (28) and (29)

$$\begin{aligned}t &= n_0\frac{\partial\ln(u(\omega,\alpha))}{\partial(i\omega)}\bigg|_{\omega=0} = \mu x\rho_0 k_BT\frac{\partial u(\omega,\alpha)}{\partial(i\omega)}\\ &= \frac{\mu x\nu_0 e^{-\beta_{\mathrm{mid}}}(\sinh(\zeta)/\zeta)}{(\alpha-\nu_0e^{-\beta_1})(\alpha-\nu_0e^{-\beta_2})}. \end{aligned}\quad (31)$$

Some notations are used for short. They are $\beta_{1,2} = W_{1,2}/(k_BT)$, $\beta_{\mathrm{mid}} = (\beta_1+\beta_2)/2$, and $\zeta = (\beta_2-\beta_1)/2$. Hence, for the fitting parameter, we get

$$\alpha = \nu_0 e^{-\beta_{\mathrm{mid}}}\cosh(\zeta) - \nu_0\sqrt{\frac{\mu x}{\nu_0 t}\frac{\sinh(\zeta)}{\zeta}e^{-\beta_{\mathrm{mid}}}+e^{-2\beta_{\mathrm{mid}}}\sinh^2(\zeta)}. \quad (32)$$

The change in time and the $\rho(x,t)$-coordinate in this case is similar to the (14) distribution (see Fig. 3). There is some difference in the speed of the particle train propagation as (33), shown at the bottom of the page. The $\rho_0(x,t)$ coefficient is defined as it was before by expressions u_0 and σ^2, and because of its bulkiness, its explicit form is not given. The study on the extremum of expression (33) allows to calculate the propagation speed of the particle train. In this case, the expression for speed is given as follows:

$$V = \frac{\nu_0}{\mu}\frac{\zeta}{\sinh(\zeta)}e^{-\beta_{\text{mid}}} = \frac{\nu_0}{2\mu k_B T}\frac{\exp(-(W_2+W_1)/(2k_BT))}{\sinh((W_2-W_1)/(2k_BT))}(W_2-W_1). \quad (34)$$

Without fluctuations of the ($\zeta = 0$) energy, limiting case (34) can be obtained from formula (15). The dependence of velocity (34) on the ζ parameter, i.e., on the value of the random activation energy spread, needs a comment. As ζ increases, the speed of the wall decreases. This effect can be explained by the following qualitative considerations. Due to the exponential dependence of the frequencies ν on β, the main contribution to the resulting time for a quasiparticle to reach a certain coordinate x is made by high barriers. The vortices cores spend much time on such centers of anchoring. We can see that the lower the temperature, the stronger the sampling effect. At low temperatures, even small differences in the (W_2-W_1) activation energies result in catastrophic differences in the lifetimes at the barriers. In the limit of the ζ maximum, when it can be assumed that the $\beta_2 \gg \beta_1$ expression for the velocity takes the form

$$V \approx \frac{\nu_0}{\mu}\beta_2 e^{-\beta_2} = \frac{\nu_0}{\mu}\frac{W_2}{k_BT}e^{-\frac{W_2}{k_BT}}. \quad (35)$$

Expression (35) shows that, at $T \to 0$, the motion looks as if there is only one, the most effective anchoring center in the gas path, where the lifetime determines the average velocity of the vortex.

To estimate the time dependence on the degree of the coordinates hardcover of the vortices cores, it is necessary to repeat procedure (15)–(17) with calculated parameter (32). By using the $\Delta x \ll Vt$ assumption, the expression is obtained

$$\sigma_x^2 \approx 16\ln(2)\frac{\nu_0 t e^{-\beta_{\text{mid}}}}{\mu^2}\frac{\zeta^2\cosh(\zeta)}{\sinh^2(\zeta)} = 16\ln(2)\frac{\nu_0 t}{\mu^2}\left(\frac{W_2-W_1}{2k_BT}\right)^2\exp\left(-\frac{W_2+W_1}{2k_BT}\right)\times\cosh\left(\frac{W_2-W_1}{2k_BT}\right)\left(\sinh\left(\frac{W_2-W_1}{2k_BT}\right)\right)^{-2}. \quad (36)$$

With the growth of the ζ range, where the heights of the energy barriers fluctuate, the dispersion of the coordinates of the quasiparticles behaves nonmonotonically. This effect will be discussed later in Section V.

The above circumstances indicate the need to consider the random nature of the fixing field in the theoretical description of the processes of vortices/skyrmions motion. It is especially important at low temperatures.

IV. Normal Activation Energy Distribution (Model 3)

In this section, another special case of the model distribution of the activation energy in the range from 0 to ∞ according to the law is considered

$$\rho(W) = r_0\exp\left(-\frac{(W-W_0)^2}{2\sigma_W^2}\right), \quad r_0 = \frac{2}{\sqrt{2\pi\sigma_W^2}\left(1+\text{Erf}\left(W_0/\sqrt{2\sigma_W^2}\right)\right)}. \quad (37)$$

W_0 is the most probable value of the height of the defects potential barrier. σ_W^2 is the dispersion of the binding energy. Then, for function (22), we get

$$u(\omega,\alpha) = r_0\int_0^\infty \frac{\nu_0 e^{-\frac{W}{k_BT}}e^{-\frac{(W-W_0)^2}{2\sigma_W^2}}}{\nu_0 e^{-\frac{W}{k_BT}} - (i\omega+\alpha)}dW = \frac{2A}{\sqrt{\pi}(1+\text{Erf}(A\beta_0))}\int_0^\infty \frac{e^{-A^2(\beta-\beta_0)^2}}{1-\eta e^{\beta}}d\beta. \quad (38)$$

The introduced notations are $\beta = W/(k_BT)$, $\beta_0 = W_0/(k_BT)$, $A^2 = (k_BT)^2/(2\sigma_W^2)$, and $\eta = (i\omega+\alpha)/\nu_0$.

It is not possible to perform calculation (38) in general form for a wide temperature range. Therefore, the extreme cases of high and low temperature are considered. $A^2 \to 0$ is the low-temperature limit, where the denominator in integrand (38) is a much faster function of β than the numerator, and with a clear maximum at $\eta e^{\beta} = 1$. In this case, the "slow" function can be taken out of the integral sign as an ordinary constant with the β value that corresponds to the zero value of the denominator. Then, the expression for u can be presented as

$$u = \frac{2A}{\sqrt{\pi}(1+\text{Erf}(A\beta_0))}e^{-A^2(\ln(\eta)+\beta_0)^2}\int_0^\infty\frac{1}{1-\eta e^{\beta}}d\beta = \frac{2A}{\sqrt{\pi}(1+\text{Erf}(A\beta_0))}e^{-A^2(\ln(\eta)+\beta_0)^2}\ln\left(\frac{\eta-1}{\eta}\right). \quad (39)$$

With the expression for the equation of the α fitting parameter, we get (28)

$$\nu_0 t = \frac{\mu x}{\eta}\frac{2Ae^{-A^2(\ln(\eta)+\beta_0)^2}}{\sqrt{\pi}(1+\text{Erf}(A\beta_0))}$$

$$\rho(x,t) = \rho_0(x,t)\exp\left(-\mu x - \nu_0 t e^{-\beta_{\text{mid}}}\cosh(\zeta) + \sqrt{\mu x\nu_0 t\frac{\sinh(\zeta)}{\zeta}e^{-\beta_{\text{mid}}} + \left(\nu_0 t e^{-\beta_{\text{mid}}}\sinh(\zeta)\right)^2}\right.$$
$$\left. + \frac{\mu x}{2\zeta}\ln\left(\frac{\left(\frac{\mu x}{\nu_0 t}\frac{\sinh(\zeta)}{\zeta}e^{-\beta_{\text{mid}}} + e^{-2\beta_{\text{mid}}}\sinh^2(\zeta)\right)^{\frac{1}{2}} + e^{-\beta_{\text{mid}}}\sinh(\zeta)}{\left(\frac{\mu x}{\nu_0 t}\frac{\sinh(\zeta)}{\zeta}e^{-\beta_{\text{mid}}} + e^{-2\beta_{\text{mid}}}\sinh^2(\zeta)\right)^{\frac{1}{2}} - e^{-\beta_{\text{mid}}}\sinh(\zeta)}\right)\right). \quad (33)$$

$$\times\left(\frac{1}{\eta-1}-2A^2(\ln(\eta)+\beta_0)\ln\left(\frac{\eta-1}{\eta}\right)\right). \quad (40)$$

The η parameter should be taken at $\omega=0$. If the smallness of A^2 for (40) is considered, we can get

$$\frac{\nu_0 t}{\mu x}=\frac{\varphi}{\eta(\eta-1)}$$

$$\varphi=\frac{2k_BTe^{-\frac{W_0^2}{2\sigma_W^2}}}{\sqrt{2\pi\sigma_W^2}\left(1+\mathrm{Erf}\left(W_0/\sqrt{2\sigma_W^2}\right)\right)}. \quad (41)$$

Having solved the equation, we have

$$\alpha=\nu_0\eta=\frac{1}{2}\nu_0\left(1-\sqrt{1+4\frac{\mu x}{\nu_0 t}\varphi}\right). \quad (42)$$

With α for the u_0 value (39), we can have

$$u_0\approx\varphi\ln\left(\frac{\sqrt{1+4\mu x\varphi/(\nu_0 t)}+1}{\sqrt{1+4\mu x\varphi}/(\nu_0 t)-1}\right). \quad (43)$$

In this case, the $\rho(x,t)$ function takes the form

$$\rho(x,t)=\rho_0(x,t)\exp\left(-\mu x-\frac{\nu_0 t}{2}\left(1-\sqrt{1+4\frac{\mu x}{\nu_0 t}\varphi}\right)+\mu x\varphi\ln\left(\frac{\sqrt{1+4\mu x\varphi/(\nu_0 t)}+1}{\sqrt{1+4\mu x\varphi/(\nu_0 t)}-1}\right)\right). \quad (44)$$

As it has been before, the study of expression (44) for the extremum determines the value of the V velocity

$$V\approx\frac{\nu_0}{\mu}\frac{e^{1-\frac{1}{\varphi}}}{\varphi}=\frac{\nu_0}{\mu}\frac{\sqrt{2\pi\sigma_W^2}}{2k_BT}\left(1+\mathrm{Erf}\left(\frac{W_0}{\sqrt{2\sigma_W^2}}\right)\right)\times\exp\left(1+\frac{W_0^2}{2\sigma_W^2}-\frac{\sqrt{2\pi\sigma_W^2}}{2k_BT}\left(1+\mathrm{Erf}\left(\frac{W_0}{\sqrt{2\sigma_W^2}}\right)\right)e^{\frac{W_0}{2\sigma_W^2}}\right). \quad (45)$$

The calculation of the half-width of the $\rho(x,t)$ function by procedure (15)–(17) with (45) and by using the $\Delta x\ll Vt$ condition allows to obtain an approximate expression for the dispersion in the low-temperature limit

$$\sigma_x^2\approx 8\ln(2)\frac{\nu_0 t}{\mu^2}\frac{e^{1-\frac{1}{\varphi}}}{\varphi^2}\left(1+4e^{1-\frac{1}{\varphi}}\right)^{\frac{3}{2}}=2\ln(2)\frac{\nu_0 t}{\mu^2}\frac{2\pi\sigma_W^2}{(k_BT)^2}\left(1+\mathrm{Erf}\left(\frac{W_0}{\sqrt{2\sigma_W^2}}\right)\right)^2\times\exp\left(1+\frac{W_0^2}{\sigma_W^2}-\frac{\sqrt{2\pi\sigma_W^2}}{2k_BT}\left(1+\mathrm{Erf}\left(\frac{W_0}{\sqrt{2\sigma_W^2}}\right)\right)e^{\frac{W_0^2}{2\sigma_W^2}}\right)\times\left(1+4\exp\left(1-\frac{\sqrt{2\pi\sigma_W^2}}{2k_BT}\left(1+\mathrm{Erf}\left(\frac{W_0}{\sqrt{2\sigma_W^2}}\right)\right)e^{\frac{W_0^2}{2\sigma_W^2}}\right)\right)^{\frac{3}{2}}. \quad (46)$$

The fast function is the expression in the numerator with a maximum at $\beta=\beta_0$ in the high-temperature limit in integrand (38). Therefore, approximate expression (38) takes the form

$$u=\frac{1}{1-\eta e^{\beta_0}}\int_0^\infty\frac{A}{\sqrt{\pi}}e^{-A^2(\beta-\beta_0)^2}d\beta=\frac{1}{1-\eta e^{\beta_0}}. \quad (47)$$

If this expression for the fitting parameter is considered, we obtain the following equation:

$$\nu_0 t=\mu x e^{\beta_0}\frac{1}{\left(1-\eta e^{\beta_0}\right)^2}. \quad (48)$$

In this case for the main distribution parameters, we get

$$\alpha=\nu_0 e^{-\beta_0}\left(1-\sqrt{\frac{\mu x}{\nu_0 t e^{-\beta_0}}}\right),\quad u_0=\sqrt{\frac{\nu_0 t e^{-\beta_0}}{\mu x}}. \quad (49)$$

As a result, for the $\rho(x,t)$ function in the high-temperature limit, we have an expression that coincides with the $\rho(x,t)$ value that has been obtained before for the case δ-shaped distribution of barrier heights

$$\rho(x,t)=\rho_0(x,t)\exp\left(-\mu x-\nu_0 t e^{-\beta_0}+2\sqrt{\mu x\nu_0 t e^{-\beta_0}}\right). \quad (50)$$

The velocity of the quasiparticles gas in this case is determined by the expression

$$V=\frac{\nu_0 e^{-\beta_0}}{\mu}=\frac{\nu_0}{\mu}e^{-\frac{W_0}{k_BT}}. \quad (51)$$

The $\sigma_W^2\ll(k_BT)$ condition is satisfied at high temperature, and we get the limiting case of non-fluctuating heights of the anchoring centers barriers (15). Then, for the value of the coordinate spread and in the high-temperature limit, we have

$$\sigma_x^2\approx 16\ln(2)\frac{\nu_0 t e^{-\beta_0}}{\mu^2}=16\ln(2)\frac{\nu_0 t}{\mu^2}\exp\left(-\frac{W_0}{k_BT}\right). \quad (52)$$

V. Discussion of the Results

In this article, the problem of the coordinates distribution of the magnetic vortices array moving under the influence of a constant force in a 1-D randomly distributed field of defects in space has been solved. Defects act as anchoring centers that ensure the capture of vortices. Disruptions of magnetic vortices from such centers are provoked by thermal motion. The lifetime of the vortex on the defect is determined by the temperature and height of the energy barrier that the vortex core, as a quasiparticle, has to overcome. Thus, the consideration of the drift motion of the vortex cores means the solution of the gas motion problem of quasiparticles in a random field of linear extended anchoring centers.

Special cases of model-defined activation energy distributions are considered in detail: a δ-shaped distribution (all barrier heights are the same—model 1), a smooth distribution in a certain energy range (model 2), and a distribution given by a normal law (model 3). For these cases, analytical expressions for the most probable velocity of the vortex core are obtained. Comparative graphs of the dependence of these velocities on temperature [see formulas (15), (34), (45), and (51)] are

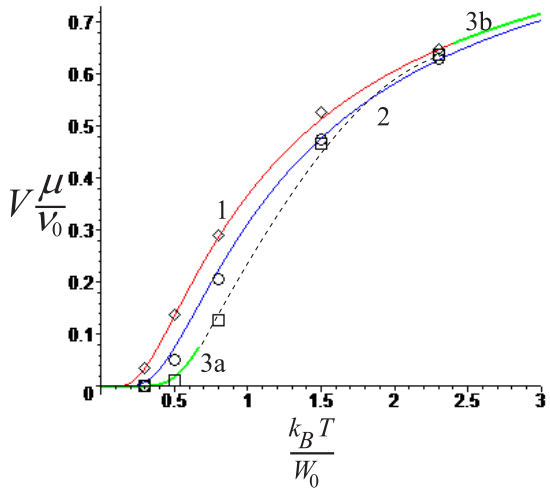

Fig. 4. Temperature dependences of the velocity displacement of the maximum coordinate of the $\rho(x,t)$ function for the models under study. Solid curve 1 means that all the heights of the energy barriers of the anchoring centers are the same. Solid curve 2 is the barrier energies are evenly distributed. Sections 3a and 3b of solid curves are the energies that are distributed according to the normal law in the low- and high-temperature ranges, respectively. At significant temperatures, curves 1 and 3b are almost indistinguishable, so graph 3b is highlighted with a thicker line. The dashed curve shows the assumed dependence of the velocity on the temperature for the normal distribution of the activation energy in the range of average temperatures ($k_BT \sim W_0$). Curve 2 shows the energy spread interval: $\Delta W = 0, \ldots, 2W_0$. Curve 3 is for the dispersion value of the energy spread: $\sigma_W^2 = W_0^2$.

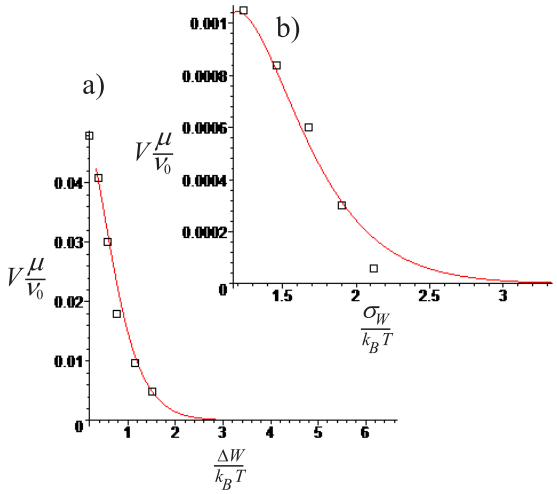

Fig. 5. Dependence of the velocity of the maximum of the $\rho(x,t)$ function on the spread interval of the energy barriers' heights. (a) Model of smooth distribution of activation energies. (b) Distribution according to the normal law.

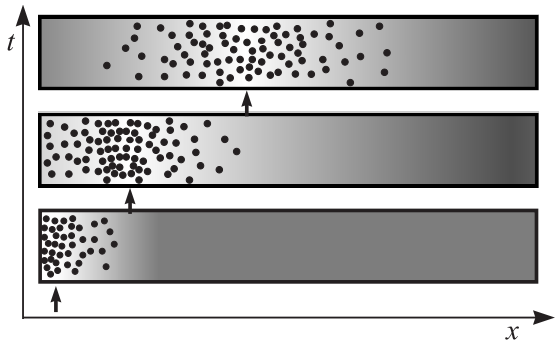

Fig. 6. Schematic representation of the evolution over time of the magnetic vortices/skyrmions concentration. The most likely coordinates at different points of time are shown by vertical arrows. In addition to shifting of the most probable coordinate, the density of quasiparticles decreases.

shown in Fig. 4. As the temperature increases, the drift velocity of the quasiparticles gas tends to $V_0 = \nu_0/\mu$, which is natural.

Fig. 5 shows the dependence of the most probable gas velocity of the vortex cores on the magnitude of the activation energies spread at fixed average energy W_0 and temperature $k_BT = 0.4W_0$. The phenomenon of a decrease in the drift velocity with increasing chaos in the activation energies for a model with a smooth distribution is explained at the end of Section III. Such arguments are even more suitable for explaining the graph in Fig. 5(b). Indeed, in a model with a normal distribution of barrier heights, the heights themselves are not limited from above, and theoretically, anchoring centers with energies significantly exceeding W_0 as the most probable value can be realized. This cannot happen in the model with a smooth distribution since the energy values of the vortex cores at specific defects cannot exceed the $2W_0$ value.

For this reason, there is the highest velocity without any chaos inside the parameters of the anchoring centers at low temperatures with comparable dispersions of models 2 and 3. Then, the speed in model 2 takes place in descending order. The lowest value of the drift velocity is obtained in model 3 for the normal energy distribution.

It is important to recall that the arguments about the significant role of rarely implemented but high barriers in model 3 are valid at low temperatures, including the context of the condition: $k_BT \ll \sigma_W$. Qualitative considerations suggest that, in the opposite case, if conditions $W_0 \gg k_BT$, $\sigma_W \ll k_BT$, and $\sigma_W \ll W_0$ are met simultaneously, model 3 should change into model 1, where there is no chaos in the activation energies. Indeed, in this case, we must consider the denominator of the integrand to be slowly changing despite the implementation of condition $W_0 \gg k_BT$ when choosing the method of approximate integration of expression (38). This can lead to the repetition of calculations (47)–(52), i.e., to results that coincide with model 1, where the barrier parameters do not fluctuate. Thus, we state the fulfillment of the natural limiting case: at $\sigma_W^2 \to 0$, model 3 changes into model 1 in a wide temperature range. Deviations that are similar to Graph 3a in Fig. 4 are realized only when the temperature tends to zero.

The increase in the spread of the vortices coordinates over time can be considered as a process similar to diffusion as a result of thermal motion, superimposed on the drift displacement with the velocities that have already been calculated (see Fig. 6). Then, the time dependence of dispersion (17), (36), (46), and (52) can be considered as the laws of diffusion in the corresponding models. In the expressions, the coefficients before the t time have the meaning of the diffusion coefficients of the vortex gas $\chi = \sigma_x^2/t$ in the defect field.

The dependence of the coefficients on the degree of the barriers' heights spread of the $\Delta W = W_2 - W_1$ anchoring centers for model 2 and σ_W^2 for model 3 is of great interest. In the high-temperature limit, there is no dependence of the diffusion coefficients on the energy spread, and for all

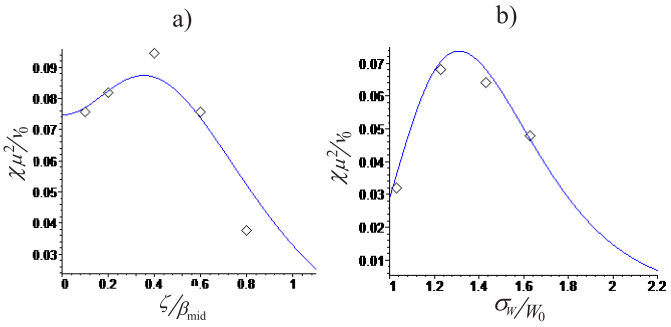

Fig. 7. Dependence of the dimensionless diffusion coefficients of the vortex gas on the value of the activation energy spread for (a) model of smooth distribution of barrier heights and (b) for the normal distribution. The curves are constructed under the following conditions: $\beta_{\text{mid}}/(k_BT) = 3$ and $W_0/(k_BT) = 3$.

models, the coefficient tends to the value: $\chi \approx 16\ln(2)\nu_0/\mu^2$. At low temperatures, we have a peculiarity like in the case of the particle train velocity V. For models 2 and 3, the χ dependences on the degree of chaos in the energies are shown in Fig. 7.

For model 3, the χ parameter at all other equal conditions has a much lower value than for model 2. We associate it with the fact that the barriers' heights spread in model 2 is clearly limited by the ΔW interval, in contrast to the normal distribution, where the realizations of energies that significantly exceed the W_0 values are possible. The realizations limit the growth rate of the gas localization region of quasiparticles over time. The property of the normal distribution also explains a more pronounced dependence $\chi(\sigma_W)$ in model 3.

An interesting fact is that the graphs in Fig. 7 are nonmonotonic. With a small value of the ($\zeta \ll \beta_{\text{mid}}$ or $\sigma_W \ll W_0$) activation energy spread, when almost all defects are the same in their effect on vortices, a slight increase in ζ and σ_W is accompanied by a natural increase in σ_x^2, as a response of the system to a more chaotic "input signal." However, with the growth of chaos in the barriers' heights of the anchoring centers at low temperatures, a significant role is played by rare but more rigid defects, where the quasiparticles gas can fix itself and slows down the expansion of its localization area. It results in the diffusion coefficients decrease. The motion of the vortices gas, in this case, looks as if most of the quasiparticles are delayed at one (several) high barrier with the growth of ζ (or σ_W), which limits the spread of coordinates and the drift velocity, which follows from (34) and (45).

VI. Conclusion

Theoretical consideration of the nature of the array motion of non-interacting magnetic vortices/skyrmions in a field of randomly located defects with random parameters has shown that this motion in the nanofilm is a stationary drift displacement of a swarm of vortices, such as a quasiparticles gas. This displacement is superimposed by a process of particle dispersal that is similar to the phenomenon of diffusion. As a result of consideration of the particle distribution function in space, analytical expressions have been obtained for the drift velocity and the diffusion coefficient depending on the temperature and the spread of the random activation energy.

In the low-temperature range, when the energy of thermal motion is much less than the average value of the energy barriers' height, the features of the dependence of the diffusion coefficient on the dispersion of the activation energy of the anchoring centers have been found, i.e., nonmonotonicity associated with the determining role of the magnet defects with the maximum value of the barrier height.

In conclusion, it is important to note that the effects discussed in this article may be of great importance in understanding the nature of the vortices/skyrmions motion in randomly inhomogeneous magnets. It is especially important to understand the processes in the context of designing devices for non-volatile information storage devices, field sensors, and other spintronics devices, where the controlled motion of vortices is supposed to be used.

Acknowledgment

This work was supported by the framework of the State Task of the Ministry of Science and Higher Education of the Russian Federation under Grant FSRZ-2020-0011.

References

[1] S.-G. Je *et al.*, "Targeted writing and deleting of magnetic skyrmions in twoterminal nanowire devices," *Nano Lett.*, vol. 21, no. 3, pp. 1253–1259, 2021, doi: 10.1021/acs.nanolett.0c03686.
[2] G. Yu *et al.*, "Room-temperature skyrmion shift device for memory application," *Nano Lett.*, vol. 17, no. 1, pp. 261–268, Jan. 2017.
[3] D. Pinna *et al.*, "Skyrmion gas manipulation for probabilistic computing," *Phys. Rev. A, Gen. Phys.*, vol. 9, no. 6, Jun. 2018, Art. no. 064018.
[4] D. A. Allwood, G. Xiong, C. C. Faulkner, D. Atkinson, D. Petit, and R. P. Cowburn, "Magnetic domain-wall logic," *Science*, vol. 309, pp. 1688–1692, Sep. 2005.
[5] M. Hayashi, L. Thomas, R. Moriya, C. Rettner, and S. S. P. Parkin, "Current-controlled magnetic domain-wall nanowire shift register," *Science*, vol. 320, pp. 209–211, Apr. 2008.
[6] S. S. P. Parkin, M. Hayashi, and L. Thomas, "Magnetic domain-wall racetrack memory," *Science*, vol. 320, no. 5873, pp. 190–194, 2008.
[7] W. Kang *et al.*, "Voltage controlled magnetic skyrmion motion for racetrack memory," *Sci. Rep.*, vol. 6, no. 1, Mar. 2016, Art. no. 23164.
[8] I. Medlej, A. Hamadeh, and F. E. H. Hassan, "Skyrmion based random bit generator," *Phys. B, Condens. Matter*, vol. 579, Feb. 2020, Art. no. 411900.
[9] M. Chauwin *et al.*, "Skyrmion logic system for large-scale reversible computation," *Phys. Rev. A, Gen. Phys.*, vol. 12, no. 6, Dec. 2019, Art. no. 064053.
[10] K. A. Omari and T. J. Hayward, "Chirality-based vortex domain-wall logic gates," *Phys. Rev. A, Gen. Phys.*, vol. 2, no. 4, Oct. 2014, Art. no. 044001.
[11] S. Luo *et al.*, "Reconfigurable skyrmion logic gates," *Nano Lett.*, vol. 18, no. 2, pp. 1180–1184, Feb. 2018.
[12] A. Fert, N. Reyren, and V. Cros, "Magnetic skyrmions: Advances in physics and potential applications," *Nature Rev. Mater.*, vol. 2, no. 7, p. 17031, Jul. 2017.
[13] W. Kang *et al.*, "A comparative cross-layer study on racetrack memories: Domain wall vs skyrmion," *ACM J. Emerg. Technol. Comput. Syst.*, vol. 16, no. 1, pp. 1–17, Jan. 2020.
[14] A. E. Ekomasov, S. V. Stepanov, K. A. Zvezdin, and E. G. Ekomasov, "Spin current induced dynamics and polarity switching of coupled magnetic vertices in three-layer nanopillars," *J. Magn. Magn. Mater.*, vol. 471, pp. 513–520, Feb. 2019.
[15] J. Müller, "Magnetic skyrmions on a two-lane racetrack," *New J. Phys.*, vol. 19, no. 2, Feb. 2017, Art. no. 025002.
[16] Y. Zhou, R. Mansell, and S. van Dijken, "Driven gyrotropic skyrmion motion through steps in magnetic anisotropy," *Sci. Rep.*, vol. 9, no. 1, p. 6525, Dec. 2019.
[17] S. Finizio *et al.*, "Control of the gyration dynamics of magnetic vortices by the magnetoelastic effect," *Phys. Rev. B, Condens. Matter*, vol. 96, no. 5, Aug. 2017, Art. no. 054438.

[18] Y. Liu, X. Huo, S. Xuan, and H. Yan, "Manipulating movement of skyrmion by strain gradient in a nanotrack," *J. Magn. Magn. Mater.*, vol. 492, Dec. 2019, Art. no. 165659.

[19] K. Y. Guslienko, "Magnetic vortex state stability, reversal and dynamics in restricted geometries," *J. Nanosci. Nanotechnol.*, vol. 8, no. 6, pp. 2745–2760, Jun. 2008.

[20] A. A. Thiele, "Steady-state motion of magnetic domains," *Phys. Rev. Lett.*, vol. 30, no. 6, p. 230, Feb. 1973.

[21] N. A. Usov and S. E. Peschany, "Magnetization curling in a fine cylindrical particle," *J. Magn. Magn. Mater.*, vol. 118, no. 3, pp. L290–L294, Jan. 1993.

[22] W. Scholz *et al.*, "Transition from single-domain to vortex state in soft magnetic cylindrical nanodots," *J. Magn. Magn. Mater.*, vol. 266, nos. 1–2, pp. 155–163, Oct. 2003.

[23] J.-Y. Kim and S.-B. Choe, "Simple harmonic oscillation of ferromagnetic vortex core," *J. Magn.*, vol. 12, no. 3, pp. 113–117, Sep. 2007.

[24] A. K. Zvezdin and K. A. Zvezdin, "Magnus force and the inertial properties of magnetic vortices in weak ferromagnets," *Low Temp. Phys.*, vol. 36, p. 826, Aug. 2010.

[25] F. G. Mertens, H. J. Schnitzer, and A. R. Bishop, "Hierarchy of equations of motion for nonlinear coherent excitations applied to magnetic vortices," *Phys. Rev. B, Condens. Matter*, vol. 56, no. 5, pp. 2510–2520, Aug. 1997.

[26] B. A. Ivanov, G. G. Avanesyan, A. V. Khvalkovskiy, N. E. Kulagin, C. E. Zaspel, and K. A. Zvezdin, "Non-Newtonian dynamics of the fast motion of a magnetic vortex," *JETP Lett.*, vol. 91, no. 4, pp. 178–182, Feb. 2010.

[27] K. Y. Guslienko, B. A. Ivanov, V. Novosad, Y. Otani, H. Shima, and K. Fukamichi, "Eigenfrequencies of vortex state excitations in magnetic submicron-size disks," *J. Appl. Phys.*, vol. 91, no. 10, p. 8037, 2002.

[28] V. A. Orlov, A. A. Ivanov, and I. N. Orlova, "On the effect of magnetostatic interaction on the collective motion of vortex domain walls in a pair of nanostripes," *Phys. Status Solidi (B)*, vol. 256, no. 10, Oct. 2019, Art. no. 1900113.

[29] I. Makhfudz, B. Krüger, and O. Tchernyshyov, "Inertia and chiral edge modes of a skyrmion magnetic bubble," *Phys. Rev. Lett.*, vol. 109, no. 21, Nov. 2012, Art. no. 217201.

[30] D. Cortés-Ortuño *et al.*, "Thermal stability and topological protection of skyrmions in nanotracks," *Sci. Rep.*, vol. 7, no. 1, p. 4060, Dec. 2017.

[31] Y. Liu and Z. Liang, "Measurement of skyrmion mass by using simple harmonic oscillation," *J. Magn. Magn. Mater.*, vol. 500, Apr. 2020, Art. no. 166382.

[32] T. Kamppeter, F. G. Mertens, E. Moro, A. Sánchez, and A. R. Bishop, "Stochastic vortex dynamics in two-dimensional easy-plane ferromagnets: Multiplicative versus additive noise," *Phys. Rev. B, Condens. Matter*, vol. 59, no. 17, pp. 11349–11357, May 1999.

[33] L. Zhao *et al.*, "Topology-dependent Brownian gyromotion of a single skyrmion," *Phys. Rev. Lett.*, vol. 125, no. 2, Jul. 2020, Art. no. 027206.

[34] R. E. Troncoso and Á. S. Núñez, "Brownian motion of massive skyrmions in magnetic thin films," *Ann. Phys.*, vol. 351, pp. 850–856, Dec. 2014.

[35] J. Miltat, S. Rohart, and A. Thiaville, "Brownian motion of magnetic domain walls and skyrmions, and their diffusion constants," *Phys. Rev. B, Condens. Matter*, vol. 97, no. 21, Jun. 2018, Art. no. 214426.

[36] T. Nozaki *et al.*, "Brownian motion of skyrmion bubbles and its control by voltage applications," *Appl. Phys. Lett.*, vol. 114, no. 1, Jan. 2019, Art. no. 012402.

[37] N. Papanicolaou and T. N. Tomaras, "Dynamics of magnetic vortices," *Nucl. Phys. B*, vol. 360, nos. 2–3, pp. 425–462, Aug. 1991.

[38] S. Komineas and N. Papanicolaou, "Skyrmion dynamics in chiral ferromagnets," *Phys. Rev. B, Condens. Matter*, vol. 92, no. 6, Aug. 2015, Art. no. 064412.

[39] V. P. Kravchuk, D. D. Sheka, U. K. Rößler, J. van den Brink, and Y. Gaididei, "Spin eigenmodes of magnetic skyrmions and the problem of the effective skyrmion mass," *Phys. Rev. B, Condens. Matter*, vol. 97, no. 6, Feb. 2018, Art. no. 064403.

[40] A. A. Ivanov, V. A. Orlov, and G. O. Patrushev, "On the properties of a stochastic magnetic structure of low-dimensional ultradisperse ferromagnets," *Phys. Met. Metallography*, vol. 102, no. 5, pp. 485–493, Nov. 2006.

[41] A. A. Ivanov and V. A. Orlov, "Scenarios of magnetization reversal of thin nanowires," *Phys. Solid State*, vol. 57, no. 11, pp. 2204–2212, Nov. 2015.

[42] C. C. I. Ang, W. Gan, and W. S. Lew, "Bilayer skyrmion dynamics on a magnetic anisotropy gradient," *New J. Phys.*, vol. 21, no. 4, Apr. 2019, Art. no. 043006.

[43] R. Tomasello, S. Komineas, G. Siracusano, M. Carpentieri, and G. Finocchio, "Chiral skyrmions in an anisotropy gradient," *Phys. Rev. B, Condens. Matter*, vol. 98, no. 2, Jul. 2018, Art. no. 024421.

[44] H. T. Fook, W. L. Gan, and W. S. Lew, "Gateable skyrmion transport via field-induced potential barrier modulation," *Sci. Rep.*, vol. 6, no. 1, Aug. 2016, Art. no. 21099.

[45] X. Liang *et al.*, "Dynamics of an antiferromagnetic skyrmion in a racetrack with a defect," *Phys. Rev. B, Condens. Matter*, vol. 100, no. 14, Oct. 2019, Art. no. 144439.

[46] M. Rahma, J. Biberger, V. Umansky, and D. Weiss, "Vortex pinning at individual defects in magnetic nanodisks," *J. Appl. Phys.*, vol. 93, p. 7429, 2003.

[47] C. Hanneken, A. Kubetzka, K. von Bergmann, and R. Wiesendanger, "Pinning and movement of individual nanoscale magnetic skyrmions via defects," *New J. Phys.*, vol. 18, no. 5, May 2016, Art. no. 055009.

[48] R. L. Compton and P. A. Crowell, "Dynamics of a pinned magnetic vortex," *Phys. Rev. Lett.*, vol. 97, Sep. 2006, Art. no. 137202.

[49] C. Song *et al.*, "Interaction between defect and skyrmion in nanodisk," 2020, *arXiv:2005.03385*.

[50] A. Derras-Chouk and E. M. Chudnovsky, "Skyrmions near defects," 2020, *arXiv:2010.14683*.

[51] V. A. Orlov, G. S. Patrin, and I. N. Orlova, "Interaction of a magnetic vortex with magnetic anisotropy nonuniformity," *J. Experim. Theor. Phys.*, vol. 131, no. 4, pp. 589–599, Oct. 2020.

[52] J. Castell-Queralt, L. González-Gómez, N. Del-Valle, and C. Navau, "Deterministic approach to skyrmionic dynamics at nonzero temperatures: Pinning sites and racetracks," *Phys. Rev. B, Condens. Matter*, vol. 101, no. 14, Apr. 2020, Art. no. 140404.

[53] C. Navau, N. Del-Valle, and A. Sanchez, "Interaction of isolated skyrmions with point and linear defects," *J. Magn. Magn. Mater.*, vol. 465, pp. 709–715, Nov. 2018.

[54] X. Liang *et al.*, "Dynamics of an antiferromagnetic skyrmion in a racetrack with a defect," *Phys. Rev. B, Condens. Matter*, vol. 100, no. 14, Oct. 2019, Art. no. 144439.

[55] D. Stosic, T. B. Ludermir, and M. V. Milošević, "Pinning of magnetic skyrmions in a monolayer Co film on Pt(111): Theoretical characterization and exemplified utilization," *Phys. Rev. B, Condens. Matter*, vol. 96, no. 21, Dec. 2017, Art. no. 214403.

[56] V. A. Orlov, G. S. Patrin, M. V. Dolgopolova, and I. N. Orlova, "Magnetic vortex near the extended linear magnetic inhomogeneity," *J. Magn. Magn. Mater.*, vol. 533, Sep. 2021, Art. no. 167999, doi: 10.1016/j.jmmm.2021.167999.

[57] C. Holl *et al.*, "Probing the pinning strength of magnetic vortex cores with sub-nanometer resolution," *Nature Commun.*, vol. 11, no. 1, p. 2833, Dec. 2020, doi: 10.1038/s41467-020-16701-y.

[58] H. Fangohr, S. J. Cox, and P. A. J. de Groot, "Vortex dynamics in two-dimensional systems at high driving forces," *Phys. Rev. B, Condens. Matter*, vol. 64, no. 6, Jul. 2001, Art. no. 064505.

[59] D. Stosic, "Numerical simulations of magnetic skyrmions in atomically-thin ferromagnetic films," Ph.D. dissertation, Teresa Bernarda Ludermir, Ciência da Computação, Universidade Federal de Pernambuco, Recife, Brazil, 2018, p. 149. [Online]. Available: https://repositorio.ufpe.br/bitstream/123456789/31432/1/TESE%20Dusan%20Stosic.pdf

[60] A. A. Ivanov and V. A. Orlov, "Simulation of the Brownian motion of the domain wall in a nonlinear force field of nanowires," *Eur. Phys. J. B*, vol. 88, no. 2, pp. 1–9, Feb. 2015.

[61] D. L. Huber, "Dynamics of spin vortices in two-dimensional planar magnets," *Phys. Rev. B, Condens. Matter*, vol. 26, no. 7, pp. 3758–3765, Oct. 1982.

[62] J. M. Kosterlitz and D. J. Thouless, "Ordering, metastability and phase transitions in two-dimensional systems," *J. Phys. C, Solid State Phys.*, vol. 6, p. 1181, Apr. 1973.

[63] A. V. Nikiforov and E. B. Sonin, "Dynamics of magnetic vortices in a planar ferromagnet," *Sov. Phys. JETP*, vol. 58, no. 2, pp. 373–378, 1983.

[64] I. V. Lobov, "Metod vychisleniya kriticheskogo proryva dislokatsiy cherez setku sluchayno raspolozhennykh neodinakovykh tochechnykh prepyatstviy," *Phys. Met. Metallography*, vol. 61, pp. 817–819, Jan. 1986.

[65] A. A. Ivanov, V. A. Orlov, and I. N. Orlova, "On the theory of the thermofluctuation motion of domain walls in nanowires," *Phys. Met. Metallography*, vol. 114, no. 8, pp. 631–641, Aug. 2013.